Rapid Report

Developmental expression of the potassium current $I_{K,n}$ contributes to maturation of mouse outer hair cells

Walter Marcotti and Corné J. Kros

Department of Physiology, School of Medical Sciences, University of Bristol, Bristol BS8 1TD, UK

(Received 30 July 1999; accepted after revision 14 September 1999)

1. The expression of K^+ currents in mouse outer hair cells (OHCs) was investigated as a function of developmental age between postnatal day (P) 0 and P26, using whole-cell patch clamp.

2. During the first postnatal week, a slow outward K^+ current ($I_{K,neo}$) was expressed by all OHCs from the apical coil of the cochlea. The amplitude of this current increased greatly between P0 and P6. Then, at the beginning of the second postnatal week, $I_{K,neo}$ decreased. At the same time, from P8 onwards, $I_{K,n}$, a K^+ current characteristic of mature OHCs, was rapidly expressed.

3. The expression of $I_{K,n}$ coincided with the onset of electromotility of the cell body of the OHCs, which could also be detected from P8 onwards and increased substantially in size thereafter.

4. $I_{K,n}$ was reversibly blocked by linopirdine, an inhibitor of members of the KCNQ family of K^+ channels, with a K_D of 0·7 μM. In the cochlea, KCNQ4 is only expressed in OHCs and is responsible for a form of non-syndromic autosomal dominant deafness. Linopirdine had no effect on other OHC K^+ currents at concentrations up to 200 μM. We conclude that ion channels underlying $I_{K,n}$ contain the KCNQ4 subunit.

5. In current clamp, depolarizing current injections from the resting potential triggered action potentials in OHCs during the first postnatal week. Thereafter, more rapid and graded voltage responses occurred from more negative resting potentials. Thus, OHCs mature rapidly from P8 onwards, and $I_{K,n}$ contributes to this maturation.

Hair cells of the organ of Corti transduce sound stimuli into electrical responses. Two different populations of hair cells are found within the mammalian cochlea: the inner hair cells (IHCs) and the outer hair cells (OHCs). In both cell types, displacements of the mechanosensitive hair bundle may activate transducer currents. The resultant receptor potentials are shaped by time- and voltage-dependent ionic conductances in the basolateral membrane (reviewed by Kros, 1996).

Considerable progress has been made recently in understanding the structural and functional development of the cochlea (reviewed by Pujol *et al.* 1998; Rübsamen & Lippe, 1998). In IHCs, the expression of a fast K^+ current that occurs around postnatal day (P) 12, the onset of hearing in mice (Romand, 1983; Ehret, 1983), contributes to their biophysical maturation (Kros *et al.* 1998). Very little is known, by contrast, about how the membrane currents of OHCs develop. The K^+ current that dominates the electrical properties of mature guinea-pig OHCs is largely activated at the resting potential and is termed $I_{K,n}$ (Housley & Ashmore, 1992; Mammano & Ashmore, 1996; Nenov *et al.* 1997). This current has not been found in neonatal mouse OHCs. In this study we investigated time- and voltage-dependent K^+ conductances expressed by mouse OHCs as a function of development between P0 and P26, with a view to understanding their role in the functional maturation of the cells.

METHODS

Tissue preparation

OHCs and some IHCs were studied in acutely dissected organs of Corti. Mice (Swiss CD-1, Charles Rivers, UK) were killed by rapid cervical dislocation and both cochleae were removed. The organs of Corti were transferred to a microscope chamber and immobilized under a nylon mesh. The composition of the extracellular solution was (mM): 135 NaCl, 5·8 KCl, 1·3 $CaCl_2$, 0·9 $MgCl_2$, 0·7 NaH_2PO_4, 2 sodium pyruvate, 5·6 D-glucose, 10 Hepes-NaOH. Amino acids and vitamins for Eagle's minimal essential medium were added from concentrates (Gibco, UK). The pH was adjusted to 7·5 and the osmolality was about 306 mosmol kg^{-1}. In some experiments, the M-current blocker linopirdine (RBI, UK) was applied through a pipette positioned close to the patched cell. In most current clamp experiments the concentration of $CaCl_2$ in the extracellular solution was increased to 5 mM; equimolar substitution of NaCl was used to

keep osmolality constant. The chamber was perfused using a peristaltic pump and mounted on an upright microscope (Zeiss ACM, Germany) with Nomarski optics (×40 water-immersion objective and ×16 eye-pieces). To expose the basolateral surfaces of the cells, a small tear was made in the epithelium with a suction pipette (tip diameter about 7 μm).

Electrical recording

Membrane currents from third-row OHCs and IHCs positioned in the apical coil of the cochlea were studied at room (20–25 °C) or near body (35–37 °C) temperature, by the whole-cell patch clamp technique using an EPC-7 or EPC-8 (HEKA, Germany). Patch pipettes (resistance in the bath, 2–3 MΩ) were pulled from soda glass capillaries and coated with wax. The intracellular solution contained (mM): 145 KCl, 3 $MgCl_2$, 1 EGTA-KOH, 5 Na_2ATP, 5 Hepes-KOH (pH 7·25, 298 mosmol kg^{-1}). Data were acquired using pCLAMP software (Axon Instruments, USA), filtered at 2·5 kHz, sampled at 5 kHz and stored on computer for off-line analysis. Current recordings were corrected off-line for linear leak. Membrane potentials were corrected for residual series resistance after compensation (0·5–4·6 MΩ) and for a liquid junction potential of −4 mV measured between pipette and bath solutions. For current clamp experiments, off-line series resistance correction was applied only if the voltage drop exceeded 1 mV. Resting potentials were measured after equilibration with the pipette solution. Unless specified, voltage clamp protocols are referred to a holding potential of −84 mV. During the first postnatal week, the leak conductance (g_{leak}) was calculated between −84 and −74 mV (activation of the outward K^+ current occurred near −50 mV) as 0·7 ± 0·5 nS ($n = 66$ cells, P0–P6). Starting from P8, however, g_{leak} (1·7 ± 1·3 nS, $n = 29$, P14–P26) was calculated at more negative potentials (typically between −114 and −124 mV), because from this time onwards K^+ currents activated negative to −100 mV. Electromotile responses were recorded with a laser differential interferometer (Géléoc *et al.* 1997); the patch pipette was attached to the base of the cells and motility was measured at the cuticular plate. Statistical comparisons of means were made by Student's two-tailed t test or, for multiple comparisons, analysis of variance (ANOVA) followed by Tukey's test, with $P < 0·05$ as the criterion for statistical significance. Means ± S.D. are reported unless otherwise indicated.

RESULTS

K^+ currents expressed by mouse OHCs

During the first postnatal week, depolarizing voltage steps caused slowly activating and partially inactivating voltage-dependent outward currents which increased in size with postnatal age (Fig. 1*A* and *B*). Only very small inward rectifier currents of a few tens of picoamps at −124 mV (I_{K1}; Marcotti *et al.* 1999) were usually recorded by applying hyperpolarizing voltage steps. From P9 onwards, depolarizing voltage steps still elicited slowly activating outward currents in all cells investigated, but a major difference from currents elicited during the first week was that they did not decay at all during the 170 ms steps (Fig. 1*C–E*). Hyperpolarizing voltage steps now elicited large inward currents in all cells (Fig. 1*C–E*). The amplitude of these inward currents increased during the second postnatal week. The inward currents commenced instantaneously and then decayed. When cells were held at −124 mV no such currents could be detected, indicating that the instantaneous inward currents reflected a current activated at the holding potential, whereas their decay was due to deactivation. This agrees with previous observations in mature guinea-pig OHCs where this current was named $I_{K,n}$ (Housley & Ashmore, 1992; Mammano & Ashmore, 1996; Nenov *et al.* 1997). At P8, the first evidence of a small $I_{K,n}$ component was found in six out of 11 cells.

The peak current–voltage (I–V) curves in Fig. 1*F* clearly show the increase in the outward current between P0 and P6 and the appearance of the inward current at P9. Activation curves were derived from tail currents at a fixed membrane potential (Fig. 1*G*, inset). The activation curves shown in Fig. 1*G* were obtained by plotting the normalized tail currents (extrapolated to the instant of the step) against the different prepulse potentials. In immature OHCs, the outward current activated at potentials close to −50 mV, whereas in OHCs older than P9 a component of the current activated negative to −100 mV. By P12 this component dominated the activation curve. Data were fitted by either a single first-order Boltzmann function:

$$I = I_{max}/\{1 + \exp[(V_{½} - V_m)/S]\},$$

or, where two components of activation were evident, the sum of two such functions. I is the tail current, I_{max} the maximal tail current, $V_{½}$ is the potential of half-maximal activation, V_m is the membrane potential of the preceding voltage step and S describes the voltage sensitivity of activation.

Reversal potentials were determined by a 170 ms conditioning pulse to about 0 mV, followed by a series of test pulses down to about −110 mV (data not shown). No significant difference in reversal potential was found when OHCs recorded during the first postnatal week (P0–P5: −77 ± 3 mV, $n = 9$) were compared with OHCs recorded later on (P16–P26: −74 ± 3 mV, $n = 9$). The reversal potentials for both groups of OHCs were close to the K^+ equilibrium potential in our experimental conditions ($E_K = -83$ mV, 23 °C), confirming the identity of the outward currents as K^+ currents.

Development of membrane properties of OHCs as a function of postnatal age

The development over time of the total outward K^+ current is shown in Fig. 2*A*. The amplitude of the current measured at 0 mV increased between P0 and P6 ($P < 0·001$; Fig. 2*A*). During the next 2 days, the size of the current decreased, dipping to a minimum at P9 ($P < 0·01$). The current then increased again during the second postnatal week due to the development of $I_{K,n}$. The growth of $I_{K,n}$ was measured in isolation as the deactivating tail currents (difference between instantaneous and steady-state inward currents) for voltage steps from the holding potential to −124 mV (Fig. 2*B*); the maximum current of about 400 pA corresponds to 8 nS of $I_{K,n}$ activated at −84 mV. Figure 2*C* shows developmental changes in cell capacitance measured from current transients to 10 mV hyperpolarizing steps from −84 mV. Figure 2*D* shows that the zero-current potential became more negative as soon as the instantaneous inward current indicative of

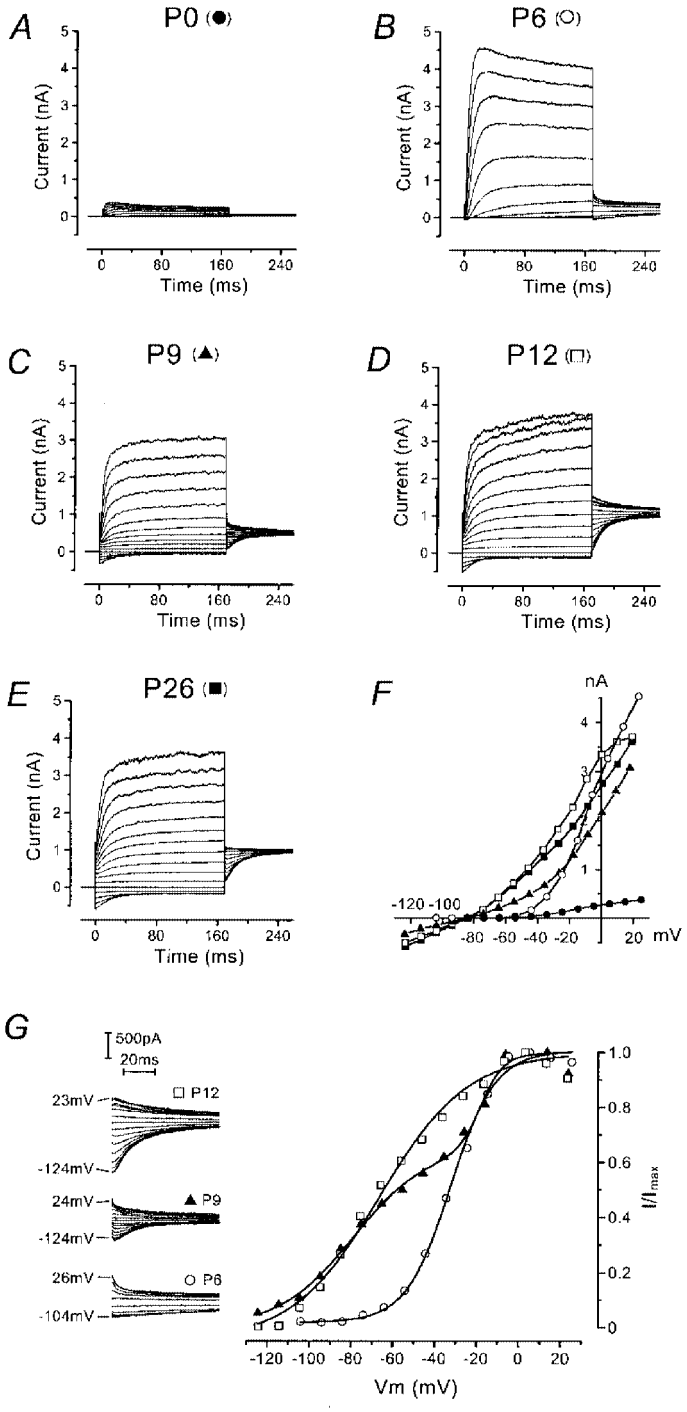

Figure 1. Outward currents in mouse OHCs during development

A–E, typical current responses from apical-coil OHCs recorded at different postnatal ages. Currents were elicited by hyperpolarizing and depolarizing voltage steps (10 mV nominal increments) from the holding potential. In this and subsequent figures, all recordings shown are single traces. Holding currents at −84 mV (plotted as zero) and leak conductances, respectively, were: P0: −16 pA, 0·2 nS; P6: −61 pA, 1·7 nS; P9: −112 pA, 0·7 nS; P12: −74 pA, 2·0 nS; P26: −54 pA, 1·4 nS. *F*, peak *I–V* curves for the OHCs shown in *A–E* (same symbols). *G*, activation curves of the outward current in three OHCs before (P6), during (P9) and after (P12) the appearance of the instantaneous inward current. The tail currents at −45 mV are shown enlarged in the inset (cells of *B*, *C* and *D*); the range of potentials of the preceding 170 ms steps is shown beside the traces. Fitting parameters for the P6 cell were: $I_{max} = 811$ pA, $V_{½} = -32$ mV, $S = 11$ mV; for the P9 cell (sum of 2 Boltzmann functions, with curve 1 contributing 65% and curve 2 35%): $I_{max} = 781$ pA, $V_{½,1} = -79$ mV, $S_1 = 18$ mV and $V_{½,2} = -18$ mV, $S_2 = 5$ mV; and for the P12 cell: $I_{max} = 1508$ pA, $V_{½} = -66$ mV, $S = 21$ mV. All recordings were at room temperature.

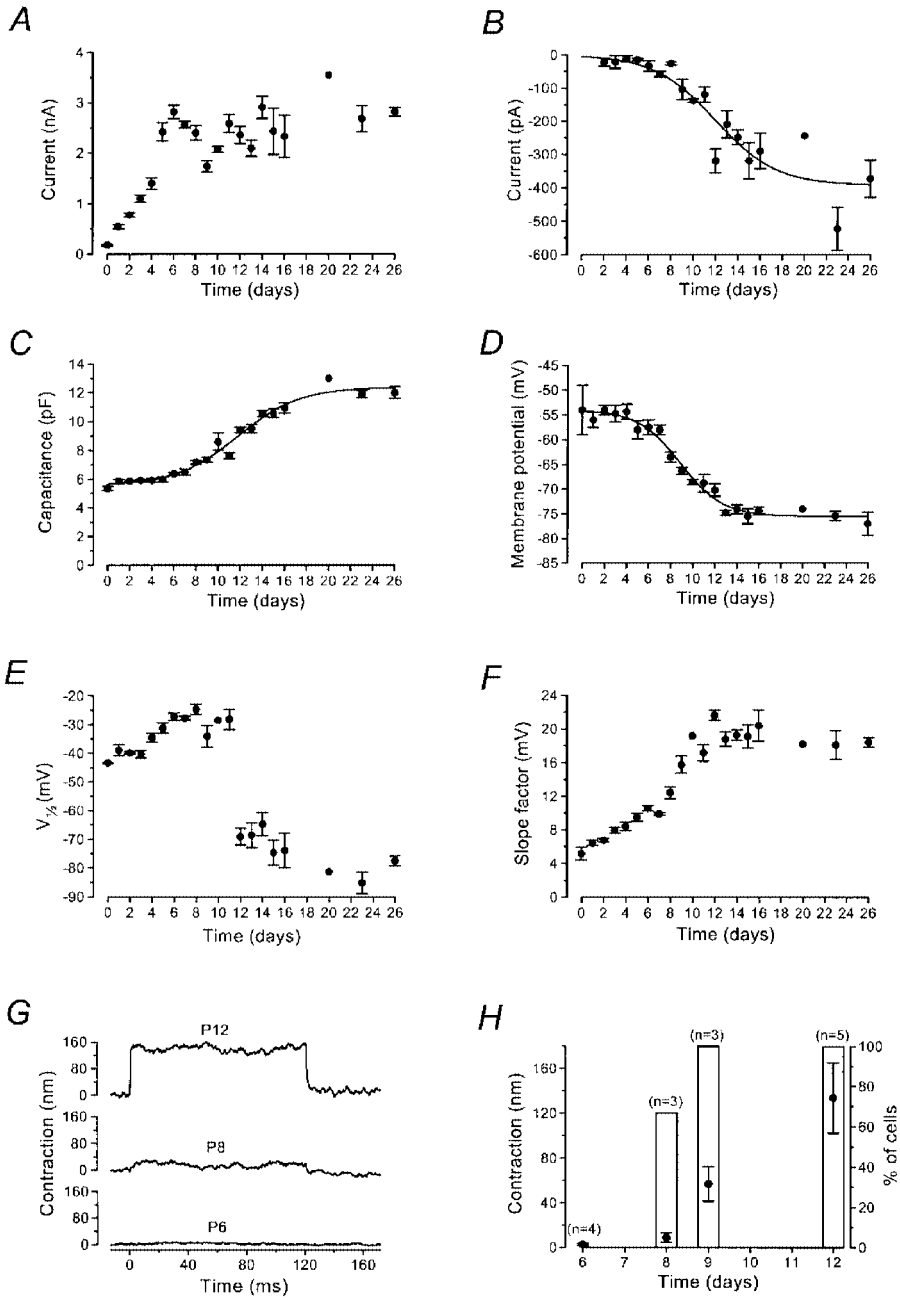

Figure 2. Development of membrane properties of mouse OHCs during maturation

A, total steady-state outward current measured at 0 mV. The number of cells measured at the various ages (P0–P26) was (from left to right): 2, 3, 29, 10, 8, 8, 6, 4, 11, 7, 2, 4, 12, 5, 11, 3, 5, 1, 5, 4. *B*, development of $I_{K,n}$. Number of cells: 6, 2, 8, 8, 2, 2, 9, 7, 2, 4, 12, 5, 11, 3, 5, 1, 5, 4. *C*, increase in membrane capacitance measured at −84 mV with age. Number of cells: 2, 3, 29, 13, 12, 8, 6, 4, 11, 7, 2, 4, 15, 5, 11, 3, 5, 1, 5, 4. *D*, zero-current potential. Number of cells: 2, 3, 29, 12, 12, 5, 4, 3, 10, 7, 2, 4, 12, 4, 11, 2, 5, 1, 5, 3. Fits to the data in *B*–*D* are according to a sigmoidal logistic growth curve:

$$A = A_{min} + (A_{max} - A_{min})/(1 + \exp(-k(t - t_{½}))),$$

where A is the size of the current, membrane capacitance or the membrane potential, k is a slope factor and $t_{½}$ is the age at which A is half-way between A_{max} and A_{min}. Values for $t_{½}$ and k, respectively, were: *B*: 11·9 days, 0·36 day^{-1}, *C*, 11·7 days, 0·36 day^{-1}; *D*: 8·9 days, 0·52 day^{-1}. *E* and *F*, half-maximal activation ($V_{½}$) and slope factor (S), respectively, for the activation curves, from fits to single Boltzmann curves. Number of cells: 2, 3, 28, 10, 8, 6, 6, 4, 8, 5, 1, 3, 12, 5, 11, 3, 5, 1, 5, 3. *G*, examples of electromotile responses to voltage steps from −64 to about +50 mV; 23 °C. *H*, development of electromotility. Left ordinate and ●: cell shortening to voltage steps from −64 to +50 mV (in nm). Right ordinate and □: percentage of cells with measurable motile responses. n, number of cells. Error bars indicate ± S.E.M. in all panels.

$I_{K,n}$ appeared (around P8–P9). The development of $V_{½}$ and slope factor of the activation curve of the total outward current (Fig. 2*E* and *F*) also suggests the gradual replacement of one conductance with another during the second postnatal week. The appearance of $I_{K,n}$ was contemporaneous with the onset of electromotility (Fig. 2*G* and *H*), characteristic of mature OHCs (Brownell *et al.* 1985; Ashmore, 1987; Santos-Sacchi & Dilger, 1988). The non-linear capacitance associated with electromotility (Santos-Sacchi, 1991) is likely to contribute a sizeable fraction of the increase in membrane capacitance at −84 mV (Fig. 2*C*) during the second postnatal week (Oliver & Fakler, 1999).

Effect of linopirdine on the K^+ currents

The M-current (I_M; Brown & Adams, 1980) blocker linopirdine (Aiken *et al.* 1995; Costa & Brown, 1997) has recently been shown to inhibit currents through KCNQ4, a novel K^+ channel subunit which in the cochlea is only expressed in OHCs (Kubisch *et al.* 1999). We tested the effects of this drug to evaluate whether KCNQ4 channels might carry one of the K^+ currents in OHCs. To assess its

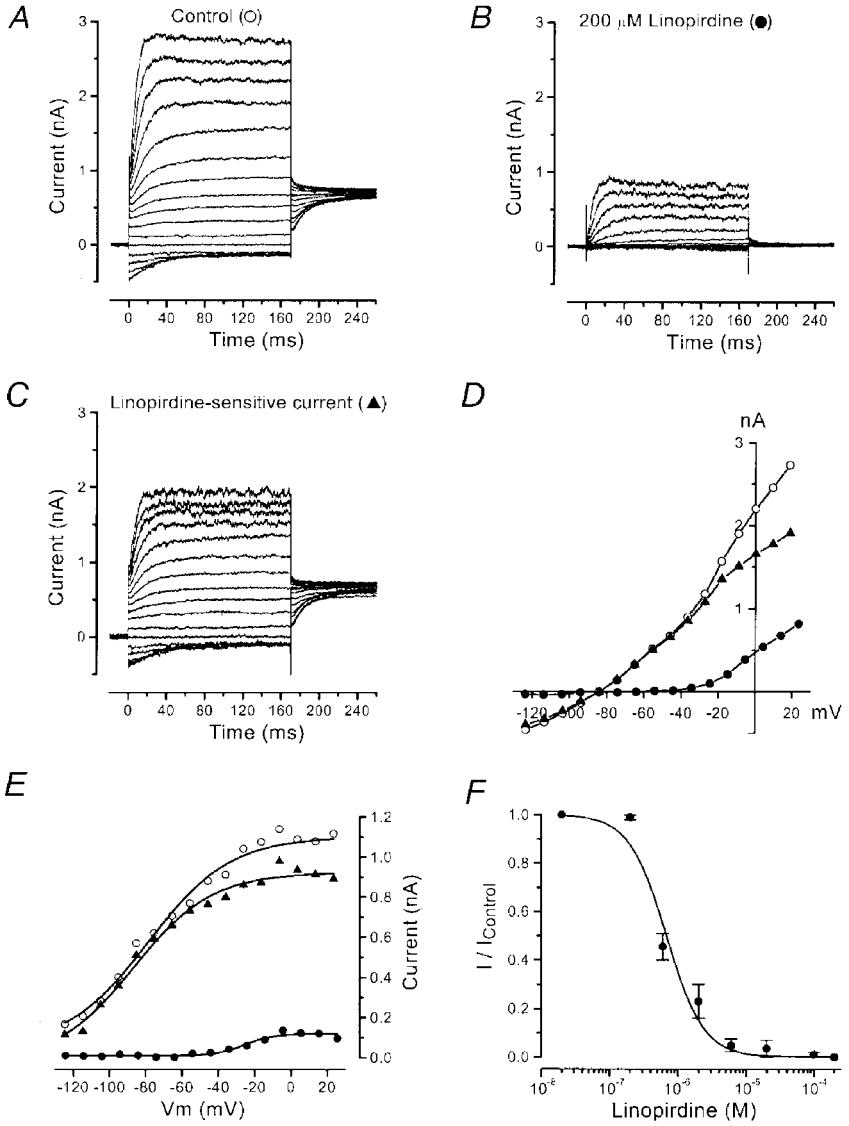

Figure 3. Effect of linopirdine on OHC currents

A and *B*, membrane currents recorded from an OHC (P12) before (*A*) and during (*B*) superfusion of 200 μM linopirdine. Holding currents, −70 pA (*A*) and −80 pA (*B*), are plotted as zero current. Leak conductance, 1·1 nS. *C*, linopirdine-sensitive current obtained by subtracting the current remaining during linopirdine treatment from the control current. *D*, peak *I–V* curves for the traces shown in *A–C* (same symbols). *E*, activation of the current before and during superfusion of 200 μM of linopirdine, from the tail currents shown in *A–C* at a constant potential of −45 mV. ○: $V_{½} = -78$ mV, $S = 22$ mV; ▲: $V_{½} = -86$ mV, $S = 21$ mV; and ●; $V_{½} = -25$ mV, $S = 8$ mV; 23 °C. *F*, dose–response curve for block of $I_{K,n}$ by linopirdine. The data were fitted to the logistic curve: $I/I_{control} = 1/(1 + ([D]/K_D)^{n_H})$, where $K_D = 0{\cdot}68 \pm 0{\cdot}10$ μM and n_H (Hill coefficient) $= 1{\cdot}6 \pm 0{\cdot}3$ (± S.E.M.). [D] is the drug concentration. Number of cells from left to right: 3, 2, 2, 2, 3, 2, 2, 6. Error bars are ± S.E.M.

selectivity (Schnee & Brown, 1998), a large concentration of 200 μM was applied to nine immature OHCs (P5), six OHCs that clearly expressed $I_{K,n}$ (age range, P12–P14) and six IHCs (P12) that already expressed the current associated with the large-conductance Ca^{2+}-activated K^+ (BK) channel, $I_{K,f}$ (Kros *et al.* 1998), all from the apical coil of the cochlea. At this concentration, linopirdine had no effect on any K^+ current in the immature OHCs or the IHCs (data not shown). By contrast, in the more mature OHCs linopirdine rapidly and completely abolished the large instantaneous inward current in response to hyperpolarizing voltage steps from the holding potential and notably reduced the outward current (Fig. 3*A* and *B*). Complete block of $I_{K,n}$ was always accompanied by a positive shift of about 20 mV of the zero-current potential. The linopirdine-sensitive current obtained by subtracting the current remaining after drug superfusion from the control current is shown in Fig. 3*C*. The effect of linopirdine was almost completely reversible after washout. The peak *I–V* curves (Fig. 3*D*) show the block of $I_{K,n}$ by linopirdine, leaving a current that activated around −50 mV, as in immature OHCs (Fig. 1*F*). The activation curves of Fig. 3*E* show that the linopirdine-sensitive current with its very negative activation range was the dominant current in mature apical-coil OHCs. The mean values ($n = 6$) for half-maximal activation ($V_{½}$) and slope factor (S) were -84 ± 12 and 23 ± 2 mV, respectively, for the control current and -86 ± 6 and 17 ± 4 mV, respectively, for the linopirdine-sensitive current. By contrast, the small outward current remaining in the presence of linopirdine activated over the same range as that of immature OHCs (Fig. 2*E* and *F*): $V_{½}$ was -30 ± 12 mV and S was 6 ± 3 mV. A dose–response curve was constructed by testing the effects of a wide range of concentrations of linopirdine on $I_{K,n}$ measured as shown in Fig. 2*B*; this is analogous to the

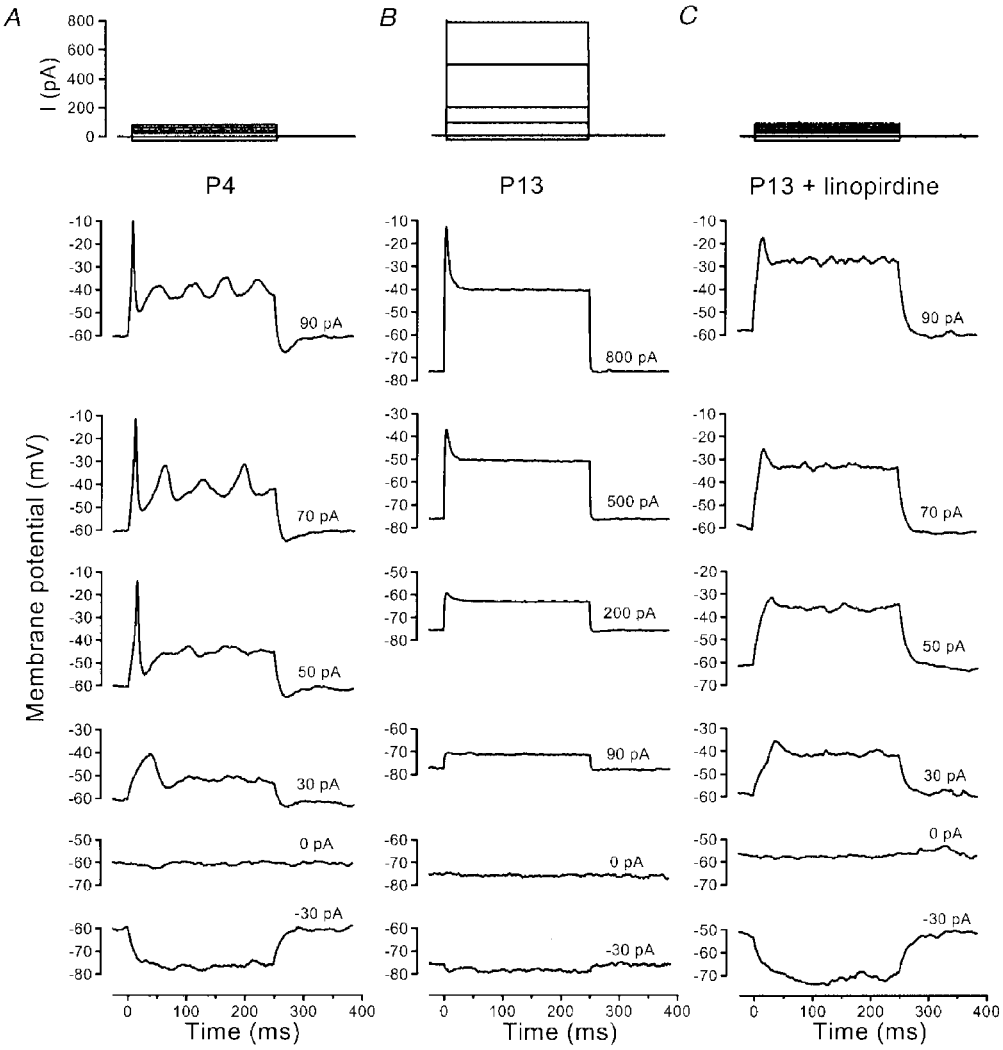

Figure 4. Voltage responses of OHCs to current injection

A, P4 immature cell. Action potentials were triggered by depolarizing current injections. Resting potential, −60 mV; 37 °C. *B*, a P13 OHC showed rapid and relatively small voltage responses around the resting potential. In addition, mature OHCs lost the ability to generate action potentials. Resting potential, −77 mV; 36 °C. *C*, voltage responses of the P13 cell shown in *B* during superfusion with 100 μM linopirdine. Resting potential was depolarized to around −60 mV. In *A–C*, recorded current steps are shown at the top.

standard method used to evaluate I_M block (Aiken *et al.* 1995). Linopirdine proved a very effective blocker of $I_{K,n}$, with a K_D of less than 1 μM (Fig. 3*F*).

Voltage responses under current clamp

The effects of the developmental changes in K^+ currents on the physiology of these cells were evaluated by current clamp experiments, all conducted at body temperature to obtain realistic voltage responses. In immature OHCs ($n = 11$, P2–P4), depolarizing current injections as small as 40 pA were able to trigger a single action potential followed by large oscillations of the membrane potential (Fig. 4*A*), in five cells investigated in the presence of 5 mM external Ca^{2+}. With 1·3 mM external Ca^{2+}, action potentials were also observed in four out of six cells but they were slower and smaller, implying a contribution of voltage-gated Ca^{2+} channels (Kros *et al.* 1993). Smaller currents usually triggered oscillations of smaller amplitude. In contrast to the immature OHCs, cells expressing $I_{K,n}$ ($n = 15$, P12–P16; all in 5 mM external Ca^{2+}) exhibited more negative resting membrane potentials and both hyperpolarizing and depolarizing current injections elicited smaller but faster responses (Fig. 4*B*). The membrane time constant for small current injections from the resting potential decreased significantly ($P < 0·001$) from $11·8 \pm 4·5$ ms ($n = 11$, P2–P4) to $1·6 \pm 0·4$ ms ($n = 15$, P12–P16). Currents larger than 100–200 pA, but well inside the range of transducer currents expected *in vivo* (up to a few nanoamps; Kros, 1996), caused the voltage to rise rapidly to a transient peak, which was followed by a steady level of depolarization (Fig. 4*B*). When mature OHCs were superfused with 100 μM linopirdine the voltage responses more resembled those of immature OHCs, but no action potentials were evident (Fig. 4*C*). This suggests that the appearance of $I_{K,n}$ contributes to the change in OHC excitability, but is not the only factor; it is conceivable that there may also be a reduction in Ca^{2+} current as OHCs lose most of their afferent innervation during maturation (Romand, 1983; Pujol *et al.* 1998).

DISCUSSION

Development of K^+ currents

The present study examines the development of K^+ currents in OHCs during maturation of the mouse cochlea. During the first postnatal week, OHCs express a delayed rectifier K^+ current that activates close to −50 mV and exhibits slow inactivation. This current, previously termed $I_{K,neo}$, is the main outward conductance in the basolateral membrane of both IHCs and OHCs before the onset of function (Kros, 1996). Recently, Kros *et al.* (1998) showed that a K^+ current ($I_{K,f}$), much larger and faster than $I_{K,neo}$, was expressed by IHCs around P12, the onset of hearing. Here we show that in OHCs profound changes in the properties of the outward K^+ conductance could be detected from P8, indicating an early maturation compared with IHCs.

In OHCs, $I_{K,neo}$ increased in size during the first postnatal week. Between P6 and P9 the total current decreased significantly, and by P8 the first signs of $I_{K,n}$, previously only described in mature guinea-pig OHCs, were detected in some cells. By P14, the current size had increased again to the level of the maximum observed at P6. This suggests that from about P6 $I_{K,neo}$ is downregulated, while the ion channels that underlie $I_{K,n}$ are inserted gradually during the second postnatal week. At this point it is not clear if the residual outward current that remains in mature OHCs in the presence of linopirdine (Fig. 3*B*) is identical to $I_{K,neo}$. It remains to be determined whether there are positional gradients in timing (as shown for electromotility; He *et al.* 1994) or magnitude (Housley & Ashmore, 1992; Mammano & Ashmore, 1996) of the expression of $I_{K,n}$ along the mouse organ of Corti: our sample of OHCs resided in a restricted part of the apical coil, with a predicted frequency range of 1–4 kHz (Ehret, 1975, his eqn (13)).

Functions of the K^+ currents

We show that immature OHCs are able to generate action potentials when depolarized beyond −40 mV from their resting potential. A previous study in neonatal rat cochlea (Oliver *et al.* 1997) showed that OHCs could fire action potentials only when held at hyperpolarized potentials near −100 mV, considerably negative to their resting potential. This discrepancy may be due either to different properties between rat and mouse OHCs or the different types of preparation used. The role of action potentials in immature OHCs is unknown at present. They are different from action potentials in IHCs, which can occur in trains and may be generated spontaneously (Kros *et al.* 1998).

The first appearance of $I_{K,n}$ in mouse OHCs at P8 coincides with the onset of electromotility, at which time we observed that the shape of the OHCs changes from ovoid to cylindrical. In the apical coil of the gerbil cochlea electromotility also starts at P8 (He *et al.* 1994). In rats, the non-linear capacitance associated with electromotility increases steeply between P5 and P10 (Oliver & Fakler, 1999). Taken together, these observations suggest that $I_{K,n}$ may contribute to a sudden biophysical maturation of OHCs well before the onset of hearing.

The present study also shows that $I_{K,n}$, the negative-activating K^+ current expressed by mature OHCs, was suppressed by extracellular application of linopirdine, a potent blocker of I_M (Costa & Brown, 1997; Schnee & Brown, 1998) flowing through KCNQ2–KCNQ3 channels (Wang *et al.* 1998). The K_D of 0·7 μM reported here for the block of $I_{K,n}$ strongly suggests that the current is similar to I_M, the only known K^+ conductance affected by such low concentrations of linopirdine (Schnee & Brown, 1998; Wang *et al.* 1998).

Recently, it has been found that 200 μM linopirdine also inhibited KCNQ3–KCNQ4 channels nearly completely; KCNQ4 homomeric channels were also blocked by linopirdine, but less effectively (Kubisch *et al.* 1999). The KCNQ channels function physiologically as heteromers. Mutations in the gene encoding KCNQ4 lead to a form of non-syndromic dominant deafness in humans (DFNA2) and

in the cochlea the mRNA is found exclusively in OHCs (Kubisch *et al.* 1999). Our results provide the first evidence that KCNQ4 is indeed expressed in the OHCs, and that it is likely to form a subunit of the channel that underlies the native OHC conductance, $I_{K,n}$, probably together with KCNQ3. The fact that mutations in this channel lead to slowly progressive hearing loss in DFNA2 patients (Kubisch *et al.* 1999) suggests that $I_{K,n}$ may be important for maintaining the viability of the cells, perhaps by virtue of the very hyperpolarized resting membrane potential that they establish and their significant activation at this resting potential. This ensures an efficient exit route for K^+ ions entering through the mechanoelectrical transducer channels of the cells. A more obvious function for $I_{K,n}$ is that it contributes to reduce the membrane time constant of OHCs to maximize the frequency response of electromotility (Housley & Ashmore, 1992; Mammano & Ashmore, 1996).

Aiken, S. P., Lampe, B. J., Murphy, P. A. & Brown, B. S. (1995). Reduction of spike frequency adaptation and blockade of M-current in rat CA1 pyramidal neurones by linopirdine (DuP 996), a neurotransmitter release enhancer. *British Journal of Pharmacology* **115**, 1163–1168.

Ashmore, J. F. (1987). A fast motile response in guinea-pig outer hair cells: the cellular basis of the cochlear amplifier. *Journal of Physiology* **388**, 323–347.

Brown, D. A. & Adams, P. R. (1980). Muscarinic suppression of a novel voltage-sensitive K^+ current in a vertebrate neurone. *Nature* **283**, 673–676.

Brownell, W. E., Bader, C. R., Bertrand, D. & De Ribaupierre, Y. (1985). Evoked mechanical responses of isolated cochlear outer hair cells. *Science* **227**, 194–196.

Costa, A. M. & Brown, B. S. (1997). Inhibition of M-current in cultured rat superior cervical ganglia by linopirdine: mechanism of action studies. *Neuropharmacology* **36**, 1747–1753.

Ehret, G. (1975). Masked auditory thresholds, critical ratios, and scales of the basilar membrane of the housemouse (*Mus musculus*). *Journal of Comparative Physiology* **103**, 329–341.

Ehret, G. (1983). Development of hearing and response behavior to sound stimuli: behavioral studies. In *Development of the Auditory and Vestibular Systems*, ed. Romand, R., pp. 211–237. Academic Press, New York.

Géléoc, G. S. G., Lennan, G. W. T., Richardson, G. P. & Kros, C. J. (1997). A quantitative comparison of mechanoelectrical transduction in vestibular and auditory hair cells of neonatal mice. *Proceedings of the Royal Society* B **264**, 611–621.

He, D. Z., Evans, B. N. & Dallos, P. (1994). First appearance and development of electromotility in neonatal gerbil outer hair cells. *Hearing Research* **78**, 77–90.

Housley, G. D. & Ashmore, J. F. (1992). Ionic currents of outer hair cells isolated from the guinea-pig cochlea. *Journal of Physiology* **448**, 73–98.

Kros, C. J. (1996). Physiology of mammalian cochlear hair cells. In *The Cochlea*, ed. Dallos, P., Popper, A. N. & Fay, R. R., pp. 318–385. Springer, New York.

Kros, C. J., Ruppersberg, J. P. & Rüsch, A. (1998). Expression of a potassium current in inner hair cells during development of hearing in mice. *Nature* **394**, 281–284.

Kros, C. J., Rüsch, A., Richardson, G. P. & Russell, I. J. (1993). Sodium and calcium currents in cultured cochlear hair cells of neonatal mice. *Journal of Physiology* **473**, 231*P*.

Kubisch, C., Schroeder, B. C., Friedrich, T., Lütjohann, B., El-Amraoui, A., Marlin, S., Petit, C. & Jentsch, T. J. (1999). KCNQ4, a novel potassium channel expressed in sensory outer hair cells, is mutated in dominant deafness. *Cell* **96**, 437–446.

Mammano, F. & Ashmore, J. F. (1996). Differential expression of outer hair cell potassium currents in the isolated cochlea of the guinea-pig. *Journal of Physiology* **496**, 639–646.

Marcotti, W., Géléoc, G. S. G., Lennan, G. W. T. & Kros, C. J. (1999). Transient expression of an inwardly rectifying potassium conductance in developing inner and outer hair cells along the mouse cochlea. *Pflügers Archiv* (in the Press).

Nenov, A. P., Norris, C. & Bobbin, R. P. (1997). Outwardly rectifying currents in guinea-pig outer hair cells. *Hearing Research* **105**, 146–158.

Oliver, D. & Fakler, B. (1999). Expression density and functional characteristics of the outer hair cell motor protein are regulated during postnatal development in rat. *Journal of Physiology* **519**, 791–800.

Oliver, D., Plinkert, P., Zenner, H. P. & Ruppersberg, J. P. (1997). Sodium current expression during postnatal development of rat outer hair cells. *Pflügers Archiv* **434**, 772–778.

Pujol, R., Lavigne-Rebillard, M. & Lenoir, M. (1998). Development of sensory and neural structures in the mammalian cochlea. In *Development of the Auditory System*, ed. Rubel, E. W., Popper, A. N. & Fay, R. R., pp. 146–192. Springer, New York.

Romand, R. (1983). Development of the cochlea. In *Development of the Auditory and Vestibular Systems*, ed. Romand, R., pp. 47–88. Academic Press, New York.

Rübsamen, R. & Lippe, W. R. (1998). The development of cochlear function. In *Development of the Auditory System*, ed. Rubel, E. W., Popper, A. N. & Fay, R. R., pp. 193–270. Springer, New York.

Santos-Sacchi, J. (1991). Reversible inhibition of voltage-dependent outer hair cell motility and capacitance. *Journal of Neuroscience* **11**, 3096–3110.

Santos-Sacchi, J. & Dilger, J. P. (1988). Whole cell currents and mechanical responses of isolated outer hair cells. *Hearing Research* **35**, 143–150.

Schnee, M. E. & Brown, B. S. (1998). Selectivity of linopirdine (DuP 996), a neurotransmitter release enhancer, in blocking voltage-dependent and calcium-activated potassium currents in hippocampal neurons. *Journal of Pharmacology and Experimental Therapeutics* **286**, 709–717.

Wang, H. S., Pan, Z., Shi, W., Brown, B. S., Wymore, R. S., Cohen, I. S., Dixon, J. E. & McKinnon, D. (1998). KCNQ2 and KCNQ3 potassium channel subunits: molecular correlates of the M-channel. *Science* **282**, 1890–1893.

Acknowledgements

This work was supported by the MRC. We thank Drs N. P. Cooper, J. C. Hancox and M. C. Holley for their comments on an earlier version of the manuscript.

Corresponding author

C. J. Kros: Department of Physiology, School of Medical Sciences, University of Bristol, University Walk, Bristol BS8 1TD, UK.

Email: c.j.kros@bristol.ac.uk